

INTERACTION OF HIGH-VELOCITY ALUMINUM SHAPED-CHARGE
JETS WITH FINITE STEEL AND CONCRETE TARGETS

David K. Davison

Physics International Company
San Leandro, California

ABSTRACT

Experiments were performed with 6.8-cm-diameter shaped charges that produced jets with tip velocities in excess of 1.0 cm/ μ s. The charges were fired at short standoff into 1-inch steel and 10-inch reinforced concrete targets, and the jets were radiographed to observe their shapes and the distributions of mass and velocity.

The experiments indicated that a mushroom-shaped jet tip can be effective in perforating hardened steel plates by the plugging process. Such jets can also be effective in perforating very thick concrete targets.

Introduction

For many applications the depth of penetration is the primary criterion for the selection of a shaped-charge design. In some cases it is desirable to create a large-diameter hole in the target. This paper describes aluminum-lined shaped charges that were specifically designed to make large holes in both steel and concrete targets. It was found that a high-velocity aluminum jet with a large-diameter tip could be effective in such an application.

Test Devices and Their Jets

Two liner shapes, designated "A" and "B," were tested. For each liner shape, two liner thickness profiles were evaluated. Figure 1 shows the test devices and the jets they produced. Table I summarizes the test results. The thickness profiles for the Type A (A1 and A2) liners were identical at the apex end of the liner; consequently, the jet tips are identical. The A1 and A2 jets were designed to have respective tail velocities of 0.82 and 0.70 cm/ μ s, respectively; the A1 liner is thicker than the A2 liner at the base end. The "lumps" in the Type A jets were not intended. They resulted from

systematic numerical errors associated with zoning boundaries in the two-dimensional hydrocode model of the shaped charges. The inner surfaces of the Type A liner were "wavy," yet the calculated jet velocity profiles were smooth. Special care was taken to reduce the influence of the zoning boundaries in the models of the Type B designs.

The B1 jet is more uniform than the Type A jet, except for a "fan" at the rear of the tip. The Type A jets had mushroom-shaped jet tips that apparently accounted for the large hole diameters in the armor plate targets. The B2 jet outline was not compared to the B1 jet outline because the B1 jet was not radiographed at a comparable time. The B2 armor target damage resembles that of the B1 jet, so it is likely that the jet tips resemble one another. The B1 liner is thicker than the B2 liner except close to the apex, where the B2 liner is thicker. The B1 and the B2 liners were designed to have the same jet velocity profiles; the B1 calculations were done with an advanced jetting algorithm.

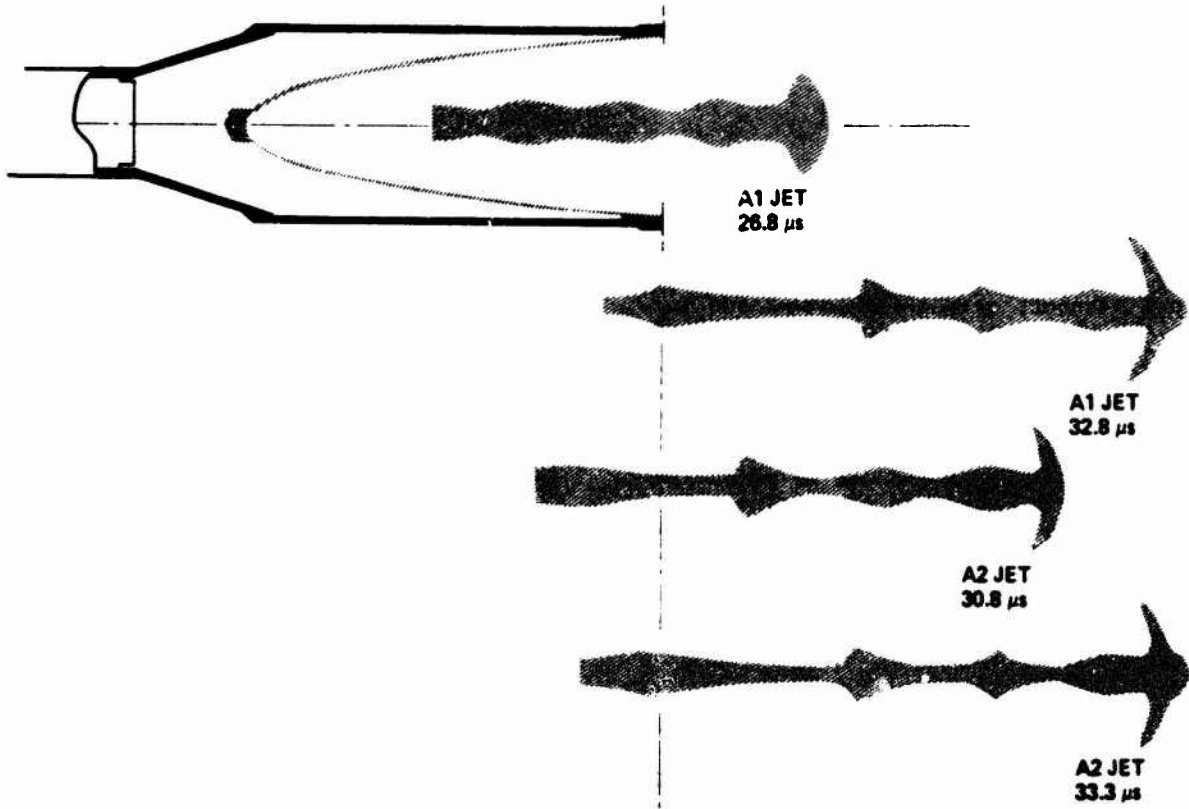
Target Damage

The charges were fired at 2-caliber standoff against 1-inch armor plates and 10-inch concrete walls. The A1 charge was fired against 4 inches of armor plate in addition to the 1-inch target. Reliable penetration data were obtained for all of the steel targets.

The Type B charges were fired into large, specially built concrete walls. The walls had crossed, 0.5-inch reinforcing bars at 12-inch intervals near both surfaces. The concrete used in the walls had a maximum aggregate size of 0.75-inch; the specification minimized the influence of the aggregate on the hole dimensions. The compressive strength was measured to be 4000 \pm 400 psi.

The A1 design was fired against a concrete slab measuring 2 feet by 2 feet

LINER SHAPE A



LINER SHAPE B

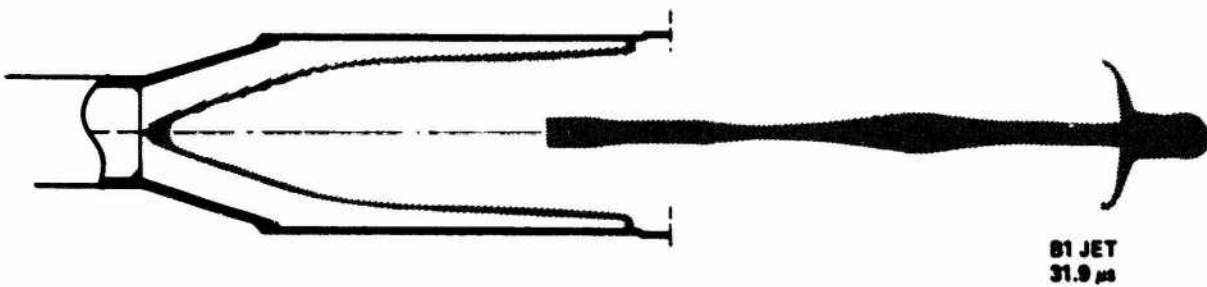


Figure 1. Warheads evaluated in test program. Liners are aluminum, 1100F, and the explosive is Octol. Times are relative to explosive initiation.

Table I. Experimental jet masses, velocities, and kinetic energies. Jet masses were calculated from jet outlines on early-time radiographs. Velocities (and experimental kinetic energies) were obtained from multiple-flash X-rays of the jets. The masses for the entries marked with asterisks (*) were derived from radiographs taken at about the same time, relative to explosive detonations. The outlines of the jets are shown in Figure 1. The estimated total kinetic energy includes the part of the jet that extended beyond the range of the radiographs.

Design	Mass (g)	Jet Velocities (cm/ μ s)		Kinetic Energy (kJ)	
		Tip	Tail	Experimental	Total
A1	5.7	1.08	0.85	326	--
* A1	6.8	--	--	--	--
A2	6.6	1.08	0.84	351	379
* A2	7.2	1.05	0.76	345	--
* B1	6.3	1.06	0.88	334	414
B2	--	0.93	--	--	--

by 10 inches. The target was so small that it was destroyed by the shot, and no reliable data are available on the performance of the design against a concrete wall. The A2 design was fired against a large slab reinforced with parallel, 1-inch reinforcing bars centered between the surfaces. The slab fractured along its length and collapsed, so the hole did not remain intact. The shape of the hole was estimated from measurements on the fractured slab.

Figure 2 shows the holes 1 inch in armor produced by the four designs; it also compares saw-cut sections of the 1-inch target and of the first inch of the 4-inch target penetrated by the A1 charge.

For the 1-inch target perforated by the A1 charge the section taken along the plane of asymmetry of the jet reveals the history of the penetration process. The left edge of the hole was formed at an earlier time than the right edge. The front surface spall, caused by the tip of the jet, is symmetrical with respect to the axis, and the right edge of the hole, further from the axis, was formed by events occurring after the impact of the tip of the jet. On impact, the bulbous jet tip (about 3 cm in diameter) fractured the target, and the remainder of the jet removed the particles created by the fracturing process. It should be noted that the defeat mechanism observed for these very hard steel targets does not necessarily apply to targets made of softer steels. Hardened steel is brittle, and the defeat mechanism depends on this

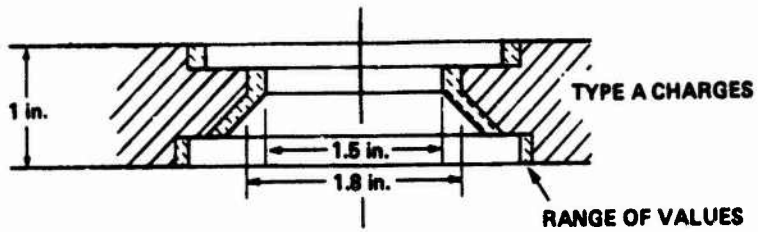
material property.

By comparison, the sectioned first inch of the thick steel target did not have a pronounced front surface spall ring, and the hole was narrower at its rear surface. The minimum hole diameter is about the same for both tests. Pronounced bending can be seen at both the front and rear edges of the first inch of the thick target. The volume of the hole created by the A1 jet in the thick steel target was 51.3 cubic centimeters.

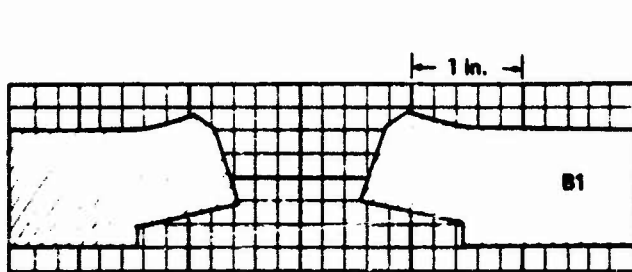
The hole shapes in concrete are illustrated in Figure 3. Perforation was accompanied by considerable spall at both surfaces of the targets. Except for the A2 test, steel witness plates were spaced behind each of the concrete targets. None of the witness plates showed evidence of jet penetration, although a small amount of aluminum vapor appeared to have been deposited on their front surfaces. The charges were centered between the reinforcing bars to minimize the hole size.

Conclusions

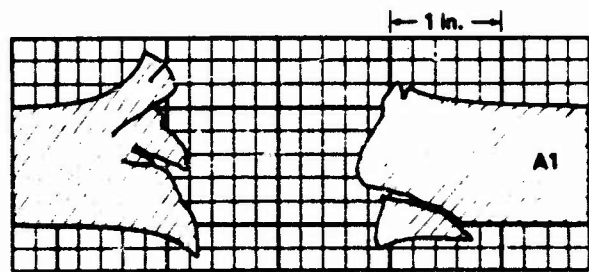
Efficient, aluminum-lined shaped charges can be designed to create large holes in both steel and concrete targets. A jet with a 3.0-cm-diameter, mushroom-shaped tip perforated a 1-inch-thick armor steel target by the plugging process, creating a hole approximately 4.0 cm in diameter. A similar jet perforated a 10-inch reinforced concrete target.



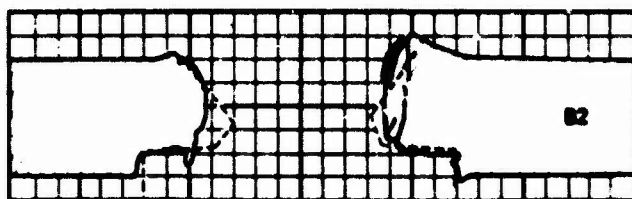
a. Cross section of holes in armor plate made by the Type A charges at 2-caliber standoff. The shape of the hole was estimated from measurements on the targets.



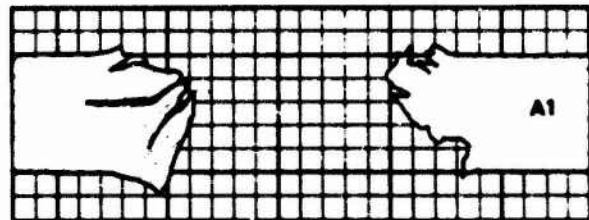
b. Cross section of the hole in the armor plate made by the B1 charge at 2-caliber standoff. The hole outline was constructed from measurements on the target.



d. Cross section of hole in the first of four armor plates, made by the A1 design at 2-caliber standoff.



c. Saw-cut section of the hole in the armor plate made by B2 charge at 2-caliber standoff. The dotted line indicates the minimum hole dimensions obtained from measurements on the target. Obviously visible fractures are shown.



e. Cross section of hole in a single armor plate, made by the A1 design at 2-caliber standoff.

Figure 2. Holes in armor.

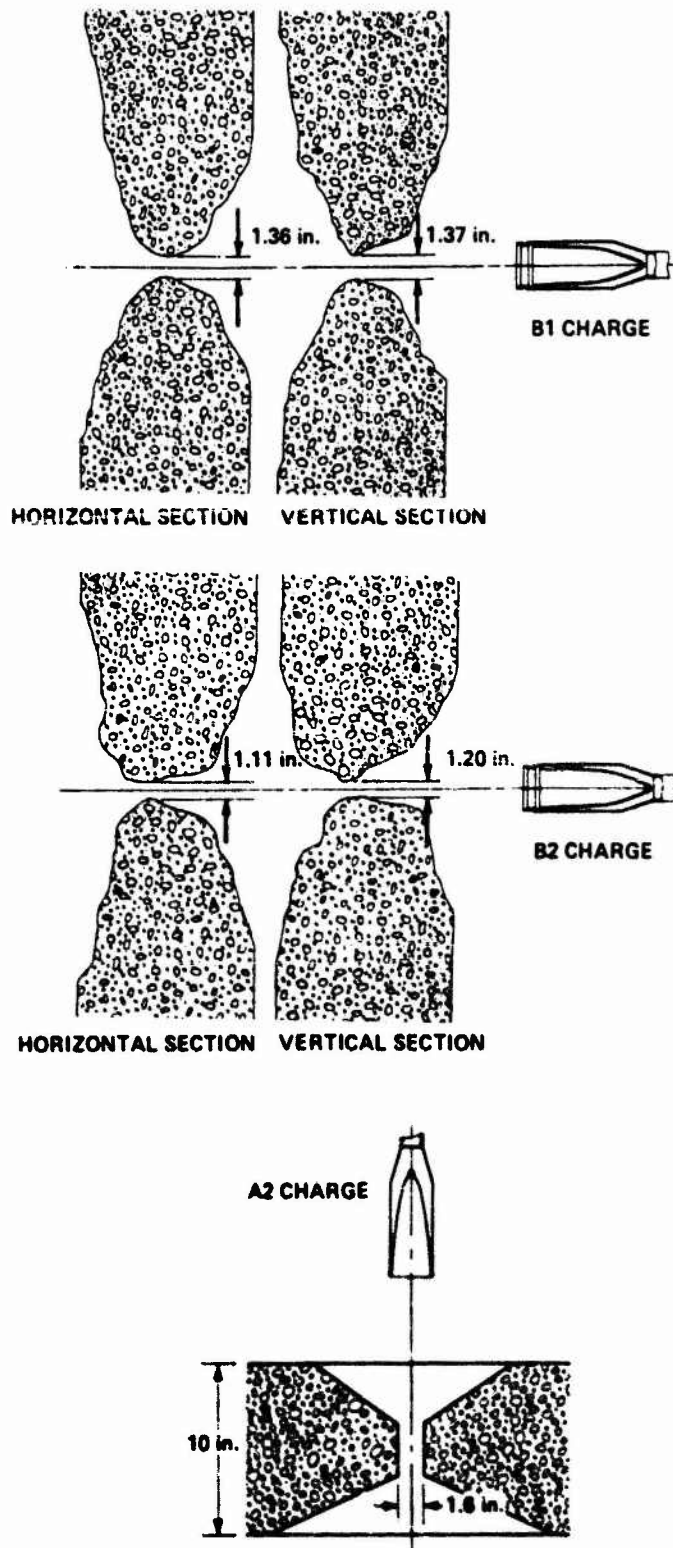


Figure 3. Holes in concrete. Nominal reinforcing bar locations are indicated.

BO-60-363